Plant Biotechnology Journal
Open Access

Plant Biotechnology Journal (2021) **19**, pp. 2082–2096 doi: 10.1111/pbi.13638

Synthesis of flavour-related linalool is regulated by *PpbHLH1* and associated with changes in DNA methylation during peach fruit ripening

Chunyan Wei[1], Hongru Liu[1,2], Xiangmei Cao[1], Minglei Zhang[1], Xian Li[1], Kunsong Chen[1] and Bo Zhang[1,*]

[1]*Laboratory of Fruit Quality Biology/Zhejiang Provincial Key Laboratory of Horticultural Plant Integrative Biology, Zhejiang University, Hangzhou, China*
[2]*Research Center for Agricultural Products Preservation and Processing, Shanghai Academy of Agricultural Sciences, Shanghai, China*

Received 6 January 2021;
revised 2 May 2021;
accepted 13 May 2021.
**Correspondence* (Tel +8657188982471; fax +8657188982224; email bozhang@zju.edu.cn)

Keywords: fruit aroma, linalool, transcription factor, epigenetics.

Summary

Linalool is one of the common flavour-related volatiles across the plant kingdom and plays an essential role in determining consumer liking of plant foods. Although great process has been made in identifying terpene synthase (TPS) genes associated with linalool synthesis, much less is known about regulation of this pathway. We initiated study by identifying *PpTPS3* encoding protein catalysing enantiomer (S)-(+)-linalool synthesis, which is a major linalool component (~70%) observed in ripe peach fruit. Overexpression of *PpTPS3* led to linalool accumulation, while virus-induced gene silencing of *PpTPS3* led to a 66.5% reduction in linalool content in peach fruit. We next identified transcription factor (TF) PpbHLH1 directly binds to E-box (CACATG) in the *PpTPS3* promoter and activates its expression based on yeast one-hybrid assay and EMSA analysis. Significantly positive correlation was also observed between *PpbHLH1* expression and linalool production across peach cultivars. Peach fruit accumulated more linalool after overexpressing *PpbHLH1* in peach fruit and reduced approximately 54.4% linalool production after silencing this TF. DNA methylation analysis showed increased *PpTPS3* expression was associated with decreased 5 mC level in its promoter during peach fruit ripening, but no reverse pattern was observed for *PpbHLH1*. Arabidopsis and tomato fruits transgenic for peach *PpbHLH1* synthesize and accumulate higher levels of linalool compared with wild-type controls. Taken together, these results would greatly facilitate efforts to enhance linalool production and thus improve flavour of fruits.

Introduction

It has been well established that volatiles, together with sugars and acids, make large contributions to fruit flavour. Lacking a characteristic or distinctive flavour is a major source of consumer dissatisfaction. Compared to content of sugars and acids at mg/g level, volatiles are presented at ng/g in fruits. Therefore, small changes in volatile content have potential to affect fruit flavour quality and there is a renewed interest to regulate fruit flavour-related volatiles (Klee and Tieman, 2018).

As a popular economic crop in the world, peach (*Prunus persica* L. Batsch) is a model plant of Rosaceae family (Zhu *et al*., 2012). More than 100 volatile chemicals have been identified in peach fruit, in which linalool is a key odorant that affects fruit aroma and consumer preference (Eduardo *et al*., 2010; Tian *et al*., 2017). Linalool, a linear monoterpene alcohol, is widely detected across 200 plant species. Due to the stereo-centre with hydroxyl at C-3, linalool has two enantiomers found in nature. R-(−)-linalool has a woody or lavender-like aroma, while S-(+)-linalool possesses sweet and floral odour (Bonnländer *et al*., 2006). S-(+)-linalool is present in seed of coriander (*Coriandrum sativum* L.), flowers of *Clarkia breweri* and sweet orange (*Citrus sinensis* Osbeck), fruit of strawberry (*Fragaria* × *ananassa* Duch) and peach. R-(−)-linalool is a major constituent of sweet basil (*Ocimum basilicum* L.), lavender (*Lavandula officinalis* L.) and bergamot orange (*Citrus aurantium* L.) (Ravid *et al*., 1985, 1997). Different neural responses of people to each enantiomeric form of linalool were observed, and therefore, each enantiomer was classified as possessing a distinct odour (Raguso, 2016).

The biosynthesis pathway of linalool has been well characterized in plants. Terpene synthases (TPSs) are the vital terminal enzymes catalysing the formation of monoterpene linalool using geranyl diphosphate (GPP) as substrate (Vranová *et al*., 2012). TPSs associated with linalool synthesis have been isolated from multiple plant species, including Arabidopsis (Chen *et al*., 2003), tobacco (He *et al*., 2019), cotton (Huang *et al*., 2017), rose (Magnard *et al*., 2018), snapdragon flowers (Nagegowda *et al*., 2008), apple (Nieuwenhuizen *et al*., 2013), grape (Martin *et al*., 2010), strawberry (Aharoni *et al*., 2004) and tomato (Falara *et al*., 2011). However, transcriptional regulation of linalool metabolism remains largely unclear. In flowers of monocotyledonous plant *Freesia hybrida*, transcription factor (TF) FhMYB21L2 activated transcription of linalool synthesis gene *FhTPS1* through binding to the MYBCORE sites in the promoter (Yang *et al*., 2020). In contrast, TF bHLH-FhMYC2 represses the transcriptional activation function of FhMYB21L2 (Yang *et al*., 2020). Extra experiments are required to further elucidate the function of these TFs in regulating linalool synthesis, including overexpressing or silencing engineering evidence. Besides, candidate TFs related to *SlTPS5* transcription were screened from tomato based on correlation analysis using a transcriptome database of stem trichome (Spyropoulou *et al*., 2014). Tomato *SlTPS5* was related to linalool formation (Falara *et al*., 2011). Although many genes related to linalool synthesis have been characterized, no TFs have

been identified to regulate linalool synthesis in fruits. Therefore, progress in identification of upstream TFs controlling volatile production lags far behind compared with fruit colour-related chemicals such as anthocyanin.

Changes in DNA methylation are essential for fruit development and ripening (reviewed by Tang *et al*., 2020), and for regulating synthesis of flavour volatiles (Zhang *et al*., 2020; Zhang *et al*., 2016). For tomato fruit in response to postharvest cold storage, volatile loss is associated with reduced expression of synthesis-related genes and increased DNA methylation levels in their promoters (Zhang *et al*., 2016). Tomatoes are harvested at mature or early ripe stage with high firmness suitable for transportation followed by exogenous ethylene to accelerate ripening. This postharvest handling caused global changes in DNA methylation status and expression of genes related to synthesis of flavour volatiles such as aldehydes, alcohols and esters (Zhang *et al*., 2020). As an important chemical related to fruit flavour, epigenetic regulation of linalool during fruit ripening remains unclear.

In the present study, RNA-sequencing results revealed that *PpTPS3* had the highest transcript abundance and correlated positively with linalool accumulation in peach fruit. Function of *PpTPS3* in regulating linalool synthesis was elucidated based on both *in vitro* evidence and *in vivo* evidence. We next identified that transcription factor PpbHLH1 activated *PpTPS3* expression via directly binding to the promoter. Correlation between gene expression and linalool content across natural cultivars was used to validate function of *PpTPS3* and *PpbHLH1* in linalool formation. In peach fruit, transient overexpressing and silencing strategies were applied to show their regulatory role in linalool synthesis. Moreover, *PpbHLH1* was stably overexpressed in model plant Arabidopsis and tomato fruits to further clarify their function in linalool production. Besides, whole-genome bisulphite sequencing was performed to analyse changes in cytosine methylation of linalool synthesis gene *PpTPS3* and *PpbHLH1* during peach fruit ripening. Taken together, we show a model of linalool regulation in peach fruit.

Results

Expression of *PpTPS3* correlates with linalool content during peach fruit ripening

Peach fruits at five developmental stages were sampled (Figure 1a) for volatile terpene production analysis using GC-MS. A total of 20 volatile terpenoids were identified in ripening peach fruit (Table S1), in which linalool was the predominant chemical (Figure 1b). Linalool production accumulated as peach fruit ripen and peaked at S5 stage, reaching up to 580.11 ng/g fresh weight and accounting for 75% of all terpenes detected in ripe peach fruit. Chiral analysis showed that approximately 70% of total linalool in ripe peach fruit was presented as S-(+)-linalool (Figure 2a). Previous study revealed that linalool is a major contributor to peach fruit aroma and flavour quality (Tian *et al*., 2017); therefore, we plan to identify genes associated with linalool synthesis and then to further investigate their regulatory mechanism.

To screen peach *TPS* genes associated with linalool synthesis, a total of 38 TPS genes displaying the HMM structure of the N-terminal conserved domain (Pfam Accession Number PF01397) and the C-terminal conserved domain (Pfam Accession Number PF03936) were identified (Figure S1; Kumar *et al*., 2018; Martin *et al*., 2010). Transcript levels of these *PpTPS* genes at five developmental stages were investigated using RNA-Seq, and 27 members expressed in peach fruit were observed (Figure 2b). Among these *PpTPS* genes, *PpTPS3* (Prupe.4G030300) and *PpTPS1* (Prupe.4G030400) had the remarkable high transcript levels during peach fruit ripening. Our previous study reported that *PpTPS1* was associated with biosynthesis of linalool, whose contents were reduced by UV-B irradiation of peach fruit after harvest (Liu *et al*., 2017). In the present study, Pearson's correlation analysis revealed a positive and significant correlation between transcript levels of *PpTPS3* and linalool contents ($R^2 = 0.902$, $P < 0.05$), indicating a potential role of this gene in linalool synthesis during peach fruit ripening. Moreover, phylogenetic tree showed that *PpTPS3* belongs to the TPS-g subfamily like other linalool synthases (Figure 2c; Table S2). As shown in Figure 2a, (S)-(+)-linalool is a major contribution to linalool in ripe peach fruit. These results prompted us to investigate whether *PpTPS3* is another candidate gene associated with linalool synthesis, particularly for (S)-(+)-linalool formation during peach fruit ripening.

Effect of overexpressing or silencing *PpTPS3* on linalool production

Full-length ORF was cloned and overexpressed in *Escherichia coli* to obtain recombinant PpTPS3 protein (Figure S2). Enzymatic activity analysis showed that PpTPS3 converted GPP to linalool (98.3% of total products) (Figure 3a). Chiral GC-MS analysis revealed that S-(+)-linalool was major products produced by PpTPS3, accounting for approximately 95% of total linalool (Figure 3a).

To our best knowledge, no transgenic peach fruits have been reported. Therefore, a homologous transient overexpression (Liu *et al*., 2017; Wu *et al*., 2019) and virus-induced gene silencing (VIGS) system (Zhao *et al*., 2020) were used to validate the function of *PpTPS3*. For transient overexpression experiments, peach fruit was infiltrated with *Agrobacterium* harbouring *PpTPS3*-pGreen-SK construct or pGreen-SK vector as control, and then, gene expression and volatile were detected after 3 d of infiltration (Figure 3b). Compared to the control, content of linalool was increased by 3.06-fold after overexpressing *PpTPS3* (Figure 3c). To confirm efficiency of VIGS system, phytoene desaturase (*PpPDS*) was used as a positive marker (Figure S3). As expected, peach fruits infiltrated with pTRV1+pTRV2-*PpTPS3* resulted in a significant reduction (~66.5%) in linalool content relative to controls (infiltrated with pTRV1+pTRV2) (Figure 3d). No significant reduction was observed for other volatiles produced by PpTPS3 protein *in vitro*. These results indicated that *PpTPS3* is involved in linalool synthesis in peach fruit.

To further test the role of *PpTPS3* in linalool formation, heterologous stable transgenic experiments were performed in Arabidopsis and tomato plants. Homozygous Arabidopsis *tps10* (SALK_041114C) mutant (Ginglinger *et al*., 2013) was used for overexpressing peach *PpTPS3*. Compared to *tps10* mutants, linalool contents were increased by 2–3 times in three independent transgenic plants (Figure 3e). Linalool accumulation in 35S::*PpTPS3*/*tps10* transgenic lines complemented linalool defect in the *tps10* mutant, even exceeded the level of wild-type Col-0 (Figure 3e). No significant changes in transcript levels were observed for *AtTPS10* and *AtTPS14*, which were associated with linalool formation, in transgenic Arabidopsis plants (Figure S4). These results revealed that the overexpression of *PpTPS3* could restore synthesis of linalool in Arabidopsis *tps10* mutant.

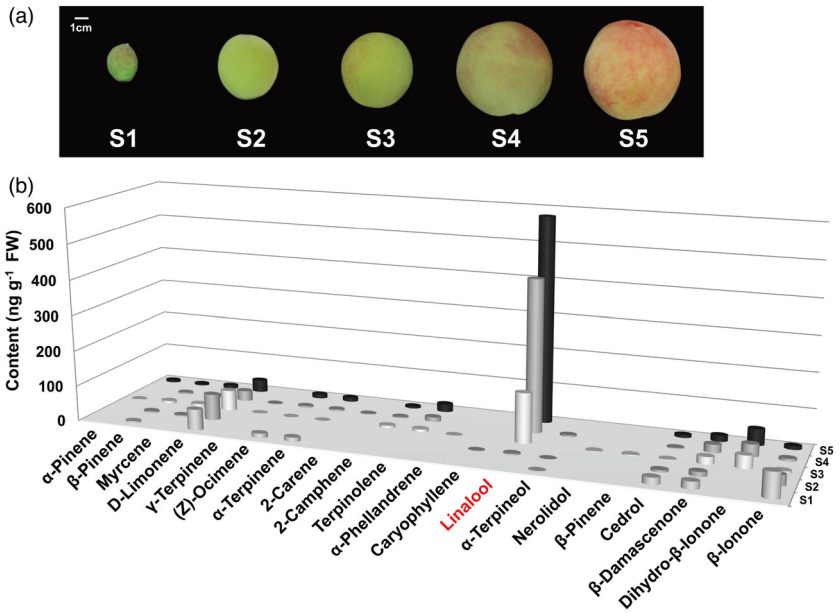

Figure 1 Changes in volatiles during peach fruit development and ripening. (a) Photo of peach fruit cv Hujingmilu at different stages: S1 (34 days after bloom, DAB), S2 (71 DAB), S3 (94 DAB), S4 (108 DAB) and S5 (111 DAB). Bars = 1 cm. (b) Volatile content of peach fruit. Averaged data from three biological replicates are shown. Standard errors are presented in Table S1.

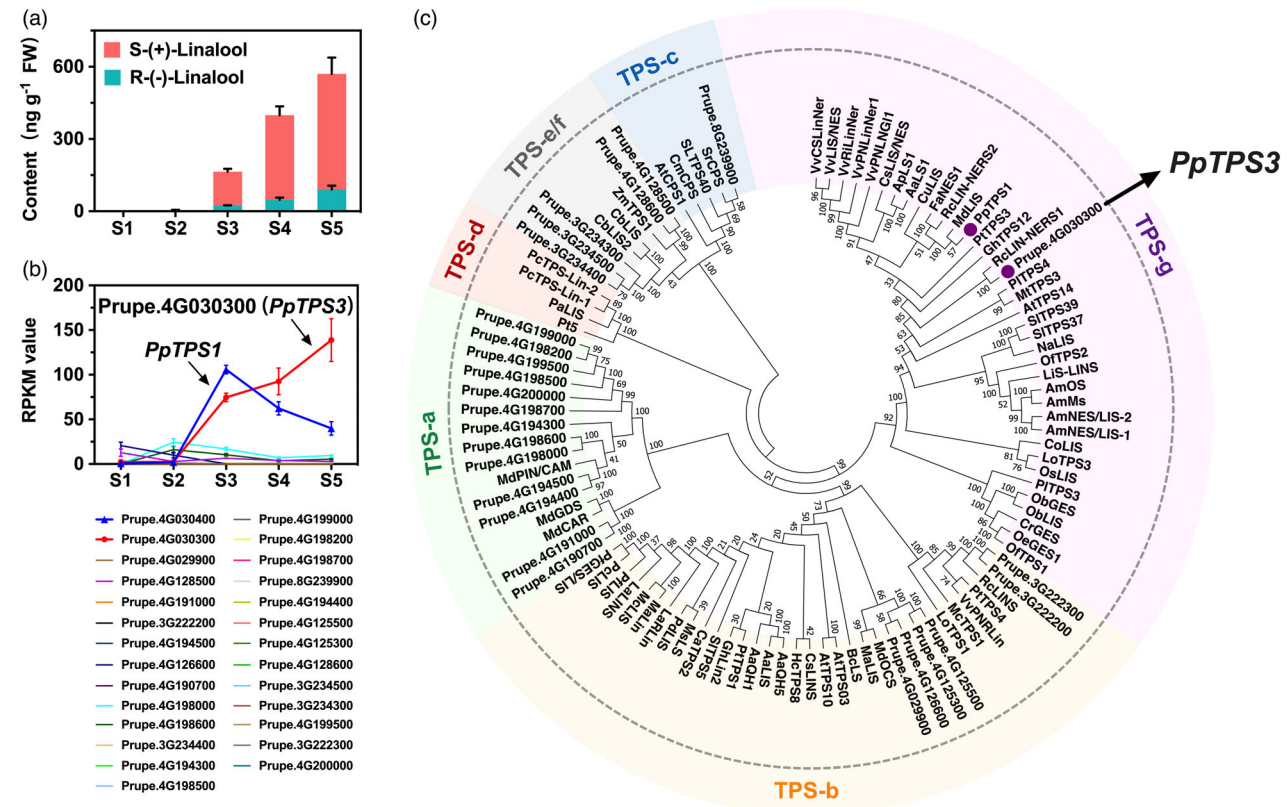

Figure 2 Characterization of *PpTPS3* related to linalool production. (a) Content of linalool during peach fruit development and ripening. The linalool enantiomers were distinguished using chiral GC–MS analysis. (b) Expression pattern of peach *TPS* genes during peach development and ripening. (c) Phylogenetic analysis of plant TPSs based on deduced amino acid sequence. Accession numbers for these TPSs are given in Table S2.

Figure 3 PpTPS3 catalyses linalool synthesis both *in vitro* and *in vivo*. (a) Enzymatic activity assay of PpTPS3 protein towards geranyl pyrophosphate (GPP) as substrate *in vitro*. (b) Schematic diagram for gene transient expression in peach fruits. (c) Transient overexpression of *PpTPS3* increases linalool content in peach fruits. Empty SK vector was used as a control. (d) Silencing *PpTPS3* by VIGS decreases linalool content in peach fruits. Empty pTRV1 + pTRV2 vector was used as a control. Phytoene desaturase (PDS) gene was used as a reporter gene for VIGS (Figure S3). (e) Overexpressing *PpTPS3* induces linalool synthesis in Arabidopsis. *tps10* mutant was used as a control. (f) Increased linalool content in tomato fruits after overexpressing *PpTPS3*. Wild-type (WT) fruits were used as controls. (g) Subcellular localization of PpTPS3. Bars = 20 μm. Data are presented as mean ± standard error from three independent biological replicates. Significant differences are indicated with asterisks above the bars (*, $P < 0.05$; **, $P < 0.01$; and ***, $P < 0.001$). N.D., not detected.

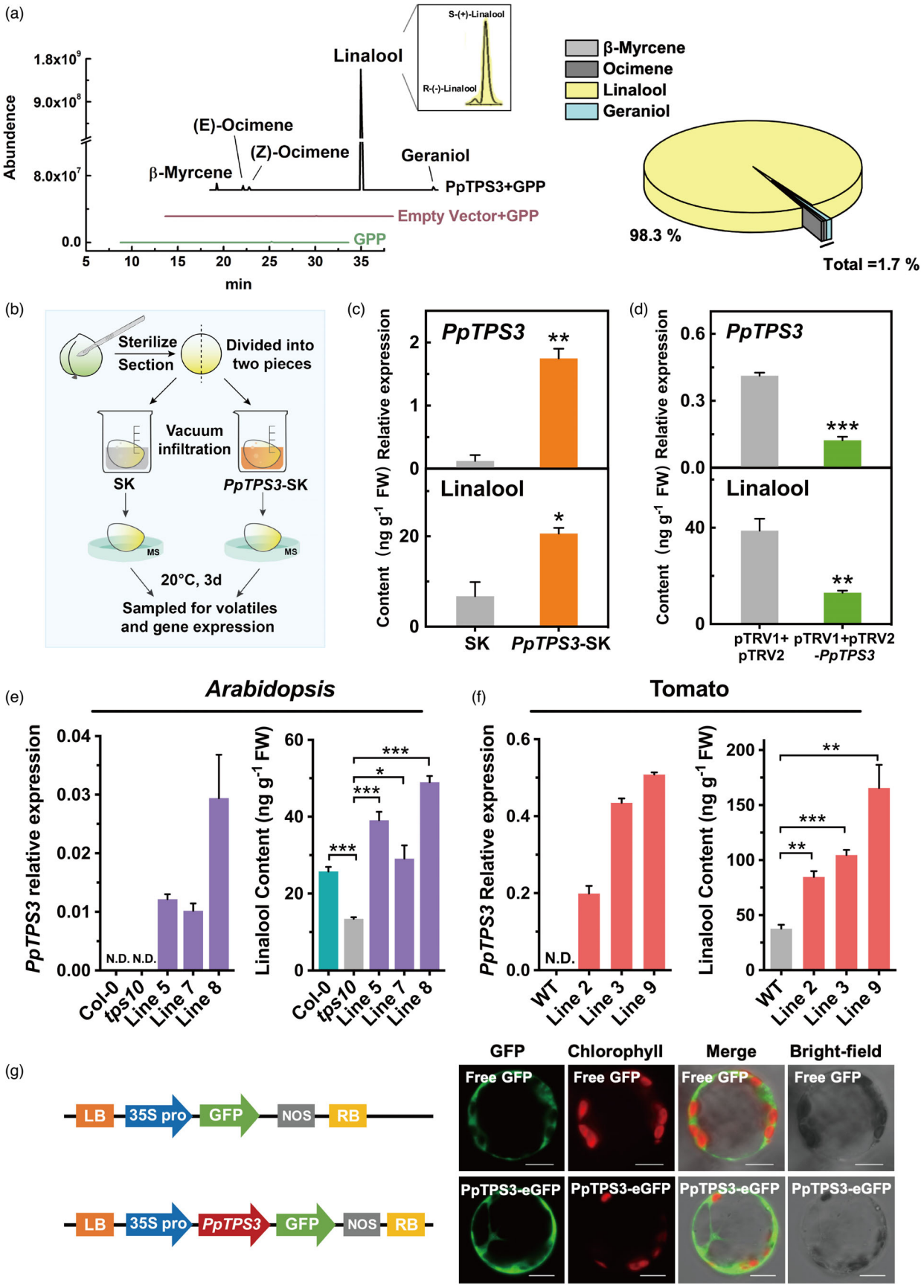

For transgenic tomatoes overexpressing *PpTPS3*, fruit at red ripe stage produced up to approximately 4.4-fold higher contents of linalool than wild-type controls (Figure 3f). Moreover, overexpressing *PpTPS3* also induced accumulation of linalool in transgenic tomato leaves (Figure S5a, b). Subcellular localization of PpTPS3 was performed in *Nicotiana benthamiana* protoplasts. The result indicated that PpTPS3 was located in the cytoplasm (Figure 3g). Taken together, results mentioned above indicated that *PpTPS3* is involved in biosynthesis of linalool in peach fruit based on both *in vitro* and *in planta* experiments.

Transcription factor PpbHLH1 activates *PpTPS3* expression via direct binding to its promoter

Having identified the gene *PpTPS3* responsible for linalool synthesis, we next investigated the regulation of its synthesis in peach fruit. Formation of volatile terpenes could be regulated by transcription factors (TFs) based on previous studies (Table S3). Therefore, homologues of these transcription factors were cloned from peach (Table S3). Besides, TFs whose expression positively correlated with *PpTPS3* in fruit ($R > 0.5$) during peach fruit ripening were also cloned for promoter activation analysis (Table S4). A total of 58 TFs, including bHLH, bZIP, ERF, MADS, MYB, NAC and WRKY families, were selected for dual-luciferase assay. Among these TFs, PpbHLH1 (Prupe.8G157500) had the strongest induction of *PpTPS3*, exhibiting approximately fourfold induction (Figure 4a). Although induction effect was also observed for PpbHLH2 (Prupe.6G211900) and PpbHLH3 (Prupe.6G212000), the highest transcript levels were detected for *PpbHLH1* during peach fruit ripening (Figure S6a). Notably, PpbHLH1 showed no transcriptional activation for *PpTPS1,* which was another gene associated with linalool formation in peach fruit (Liu *et al*., 2017; Figure S6b). Therefore, PpbHLH1 was selected as a candidate to investigate whether this TF could regulate synthesis of linalool in peach fruit.

A Y1H assay showed that PpbHLH1 could directly bind to the *PpTPS3* promoter (Figure 4b). Sequence analysis of the *PpTPS3* promoter (2000 bp) revealed that there are three bHLH binding sites, that is two E-boxes (CACATG) and one G-box (CACGTG) (Figure 4c). So, we designed three probes with 3′ biotin labelling based on these binding sites (Figure S7a), and the binding specificity of PpbHLH1 to the *PpTPS3* promoter was confirmed by EMSA. Recombinant GST-PpbHLH1 protein is shown in Figure S7b. EMSA result showed that PpbHLH1 only binds to the E-box binding site closest to the *PpTPS3* transcription start site (TSS) (Figure S7c). When the predicted binding sites were mutated, binding was eliminated (Figure 4d). With the increase in the cold probe as competitor, binding decreased. As expected, PpbHLH1 was localized in the nucleus (Figure 4e). Taken together, PpbHLH1 activated the expression of *PpTPS3* through direct binding to the E-box element in the *PpTPS3* promoter.

Expression of *PpbHLH1* correlates with linalool contents across peach cultivars

To further investigate the regulatory effects of PpbHLH1 on linalool, natural variation of gene expression and volatile contents were determined in peach cultivars (Figure 5a). The correlation between transcript level and linalool content was analysed using linear regression method. The results showed that *PpTPS3* expression strongly positively correlated with linalool content ($R^2 = 0.92$, $P < 0.001$) (Figure 5b) and S-(+)-linalool content ($R^2 = 0.93$, $P < 0.001$; Figure S8a). *PpbHLH1* expression significantly positively correlated with *PpTPS3* expression ($R^2 = 0.78$, $P < 0.01$), linalool content ($R^2 = 0.60$, $P < 0.05$; Figure 5b) and S-(+)-linalool content ($R^2 = 0.54$, $P < 0.05$; Figure S8b) among the different cultivars. Taken together, these results indicate that the expression of *PpbHLH1* is positively correlated with linalool accumulation, making PpbHLH1 a good candidate TF for regulating linalool biosynthesis in peach fruit.

Cis-acting element analysis of *PpbHLH1* promoter and its expression in response to UV-B light

Synthesis of fruit volatiles is regulated by environmental factors (Liu *et al*., 2017; Wu *et al*., 2019; Zhang *et al*., 2016). Therefore, 2000 bp of the *PpbHLH1* promoter sequence was submitted to the PlantCARE database (http://bioinformatics.psb.ugent.be/webtools/plantcare/html/) to identify *cis*-acting elements related to environmental stress (Higo *et al*., 1999). Notably, the greatest numbers of response elements were related to 'light responsiveness' in *PpbHLH1* promoter (Figure 5c), and the specific motif sequences are shown in Table S5. Our previous study revealed a regulatory role of UV-B light in linalool formation (Liu *et al*., 2017). Here, we found that transcript level of *PpbHLH1* was significantly reduced after 6 h of UV-B irradiation, followed by a decrease in *PpTPS3* expression and reduced content of linalool compared with the control (Figure 5d). Content of linalool was reduced by 60% in peach fruit after 48 h of UV-B irradiation. Our results supported a model that UV-B inhibited *PpbHLH1* expression, which in turn reduced *PpTPS3* gene transcription and linalool synthesis in peach fruit.

Effect of overexpressing or silencing *PpbHLH1* on linalool production in peach fruit

To further determine the role of PpbHLH1 on linalool synthesis, the TF was overexpressed or silenced in peach fruits using our published methods (Liu *et al*., 2017; Zhao *et al*., 2020). *PpbHLH1*-pGreen-SK vector was constructed for transient overexpression of *PpbHLH1* in peach fruit. Compared with the empty vector, overexpression of *PpbHLH1* promoted *PpTPS3* expression, accompanying by significant accumulation of linalool (Figure 6a). Chiral analysis showed that the increased linalool is mainly contributed by S-(+)-linalool (Figure 6b). VIGS significantly reduced *PpbHLH1* expression, accompanying by 53% reduction in *PpTPS3* transcript level and 54% decline of linalool production, respectively (Figure 6c). Taken together, these results indicate that *PpbHLH1* is involved in linalool production in peach fruit.

Changes in DNA methylation levels of linalool synthesis-related genes during peach fruit ripening and in response to UV-B irradiation

Epigenetic regulation is associated with fruit development and ripening (Tang *et al*., 2020), and stress responses (Zhang *et al*., 2016). To further investigate whether transcript levels of *PpTPS3* and *PpbHLH1* are associated with changes in DNA methylation, whole-genome bisulphite sequencing of peach fruit at different development stages and under UV-B treatment was performed. The average clean reads were 45.45 million, and the bisulphite conversion rates were >99.48% (Table S6). Mapping the clean reads showed that, on average 29.88 million reads (65.57%), covering >91.70% of the genome, were mapped to the peach reference genome (Tables S6 and S7). Sequencing depth was >25-fold coverage per DNA strand (Table S7). The coverage and depth of sequencing in our study are comparable with those of published fruit methylomes (Cheng *et al*., 2018; Huang *et al*.,

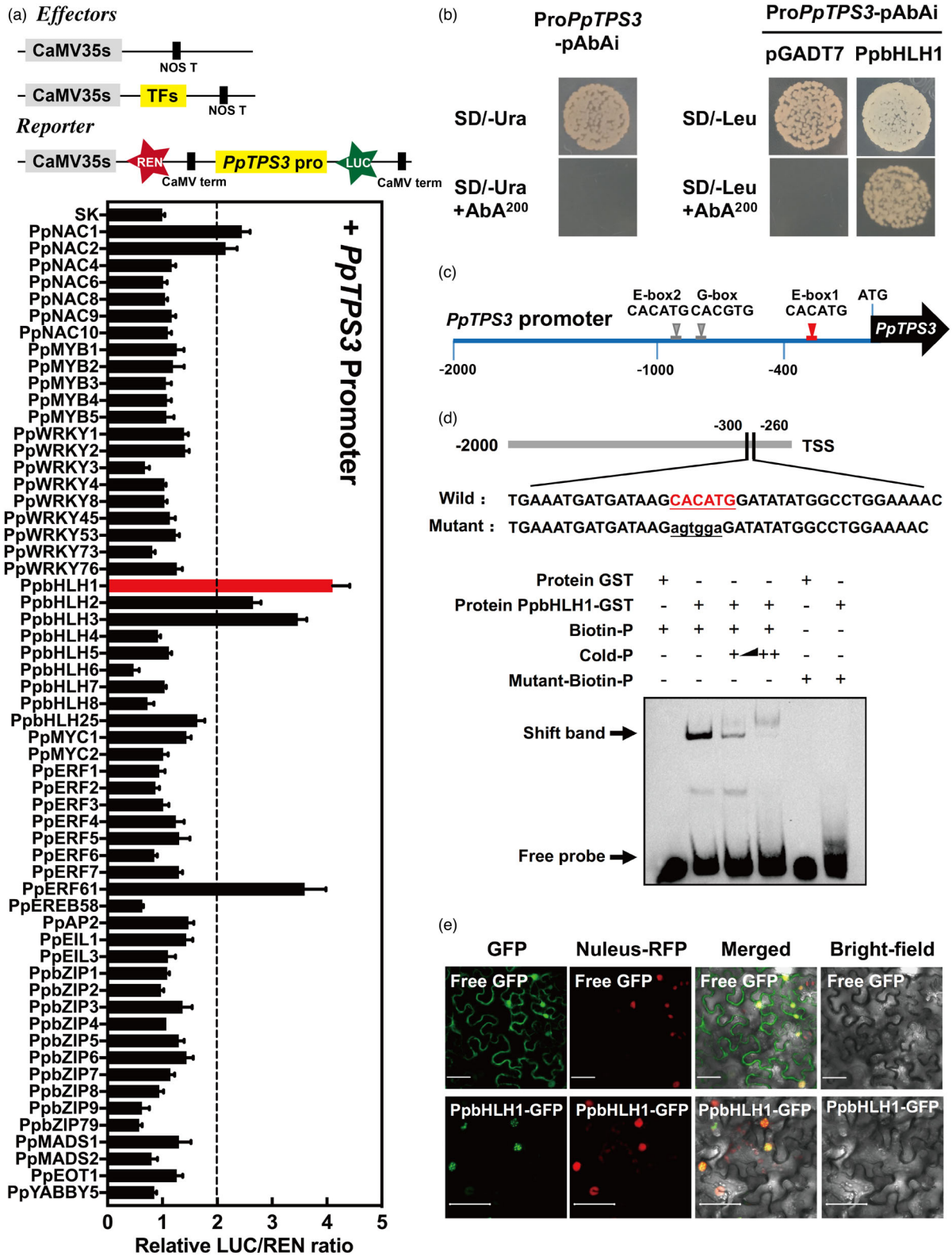

Figure 4 PpbHLH1 activates *PpTPS3* and binds to its promoter. (a) Regulatory effects of transcription factors on the promoter of *PpTPS3*. Means and standard errors were calculated from six replicates. (b) Yeast one-hybrid analysis of PpbHLH1 binding to the *PpTPS3* promoter. Autoactivation was tested on SD-Ura in the presence of AbA. AD-empty and pAbAi-*PpTPS3* were used as negative controls. (c) G-box (CACGTG) and E-boxes (CACATG) of bHLH protein-binding sites in the *PpTPS3* promoter. (d) EMSA of 3′ boitin-labelled dsDNA probes with the PpbHLH1-binding protein. Presence or absence of specific probes is marked by symbol + or -. The mutated nucleotides in probe are indicated in red lowercase letters. (e) Subcellular localization of PpbHLH1 in *Nicotiana benthamiana* leaves. GFP, GFP channel; nucleus–RFP, transgenic tobacco plants with red fluorescence in the nucleus; merge, merged image of the GFP and nucleus–RFP channels; bright-field, light microscopy image; bars = 50 μm.

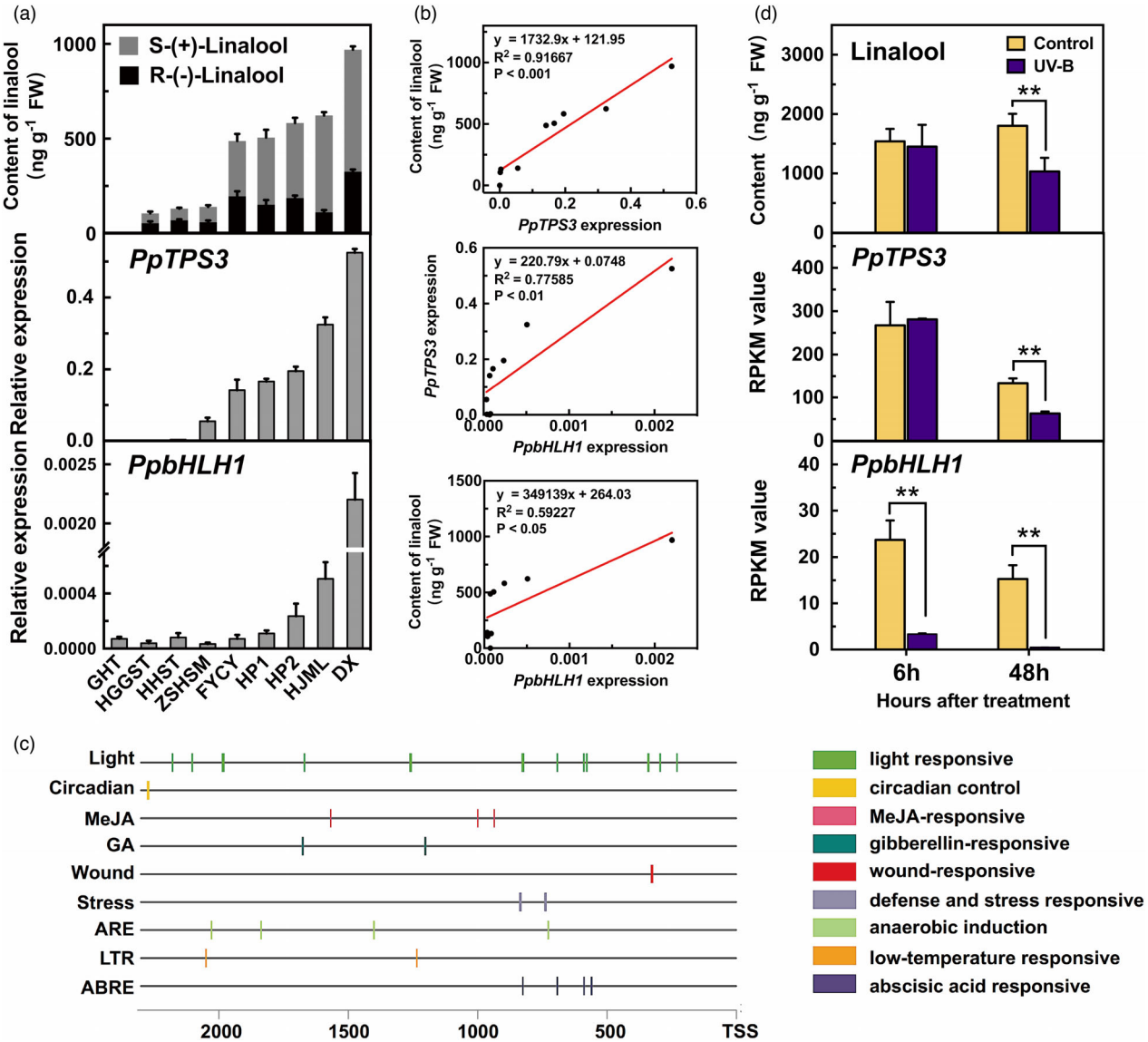

Figure 5 Correlation between transcript levels of *PpbHLH1*, *PpTPS3* and contents of linalool in peach fruit. (a) Content of linalool and expression levels of *PpTPS3* and *PpbHLH1* across peach cultivars. (b) Correlation analysis between content of linalool and expression levels of *PpTPS3* and *PpbHLH1* across peach cultivars. (c) Analysis of *cis*-acting elements of *PpbHLH1* 2kb promoter sequence based on the PlantCARE database. (d) Effect of UV-B light treatment on content of linalool and expression levels of *PpTPS3* and *PpbHLH1* in peach fruit. Relative expression levels were determined using RT-qPCR. Data are presented as mean ± standard error from three independent biological replicates. Significant differences are indicated with asterisks above the bars (**, $P < 0.01$).

2019; Xu *et al*., 2018; Zhu *et al*., 2020). A decrease in DNA methylation levels was observed for *PpTPS3* promoters throughout peach fruit development and ripening (Figure 6d). This declined DNA methylation was opposite of increased transcript levels of *PpTPS3*. Regarding *PpbHLH1*, no similar inverse pattern was observed between transcripts and cytosine methylation levels during peach fruit development and ripening (Figure 6d). For peach fruit irradiated with UV-B light, although transcript levels of *PpTPS3* and *PpbHLH1* were significantly reduced, no remarkable increase in DNA methylation levels was observed (Figure 6e). Taken together, these results indicated that decreased DNA methylation is associated with increased *PpTPS3* expression, which regulates linalool synthesis during peach fruit ripening (Figure 6f).

Figure 6 Regulatory effects of *PpbHLH1* on linalool synthesis in peach fruit. (a) Overexpressing *PpbHLH1* induces expression of *PpTPS3* and linalool accumulation in peach fruits. Empty SK vector was used as a control. Significant differences are indicated with asterisks above the bars (*, $P < 0.05$; **, $P < 0.01$; and ***, $P < 0.001$). (b) Chiral GC-MS analysis of linalool enantiomers in transiently overexpressed peach fruits. (c) Silencing *PpbHLH1* by VIGS decreases *PpTPS3* expression and linalool content in peach fruit. Empty pTRV1 + pTRV2 vector was used as a control. (d) Changes in transcript levels and DNA methylation levels of *PpTPS3* and *PpbHLH1* during peach fruit ripening. (e) Effects of UV-B irradiation on transcript levels and DNA methylation levels of *PpTPS3* and *PpbHLH1* in peach fruit. (f) A proposed regulatory model of linalool synthesis in peach fruit.

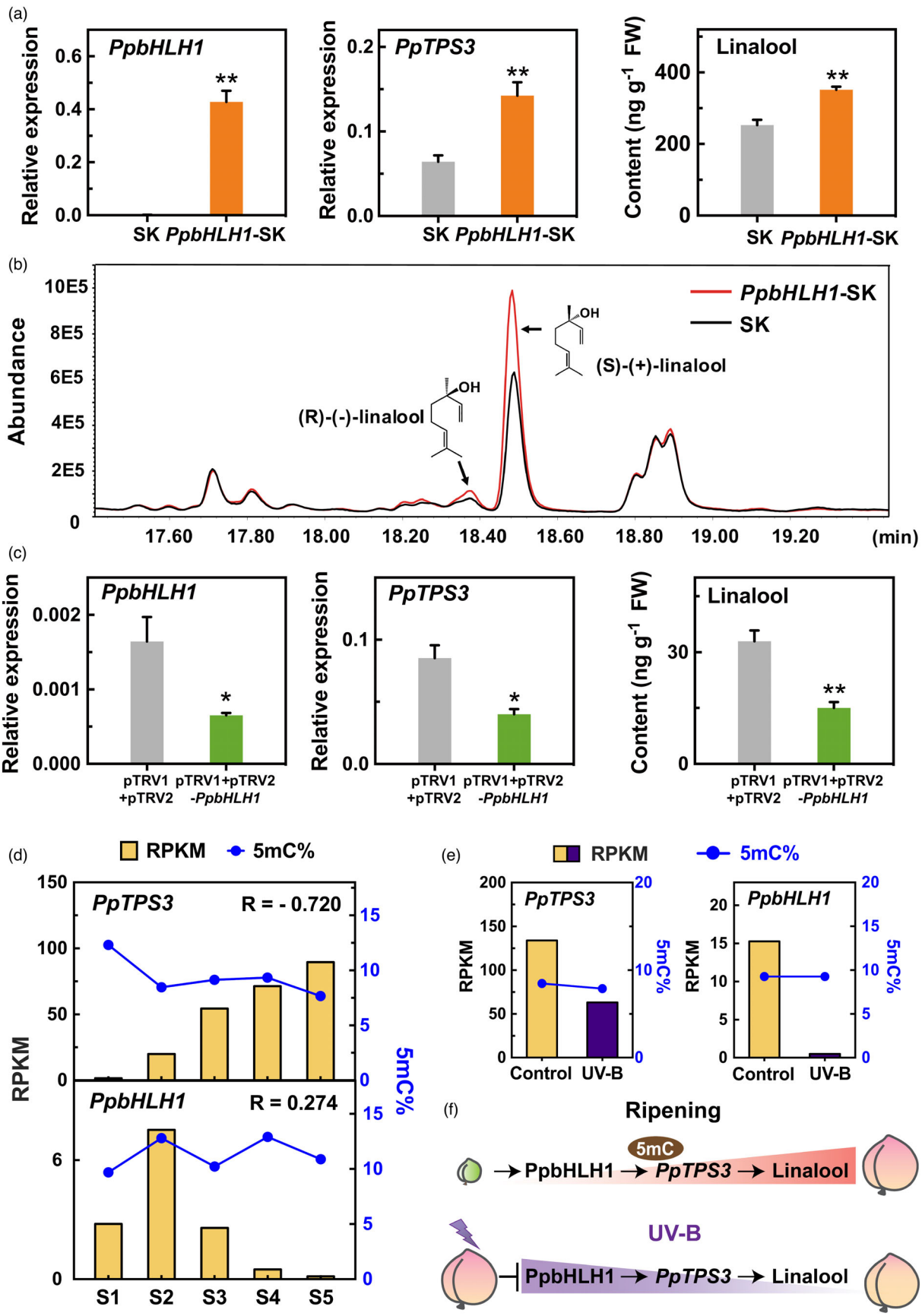

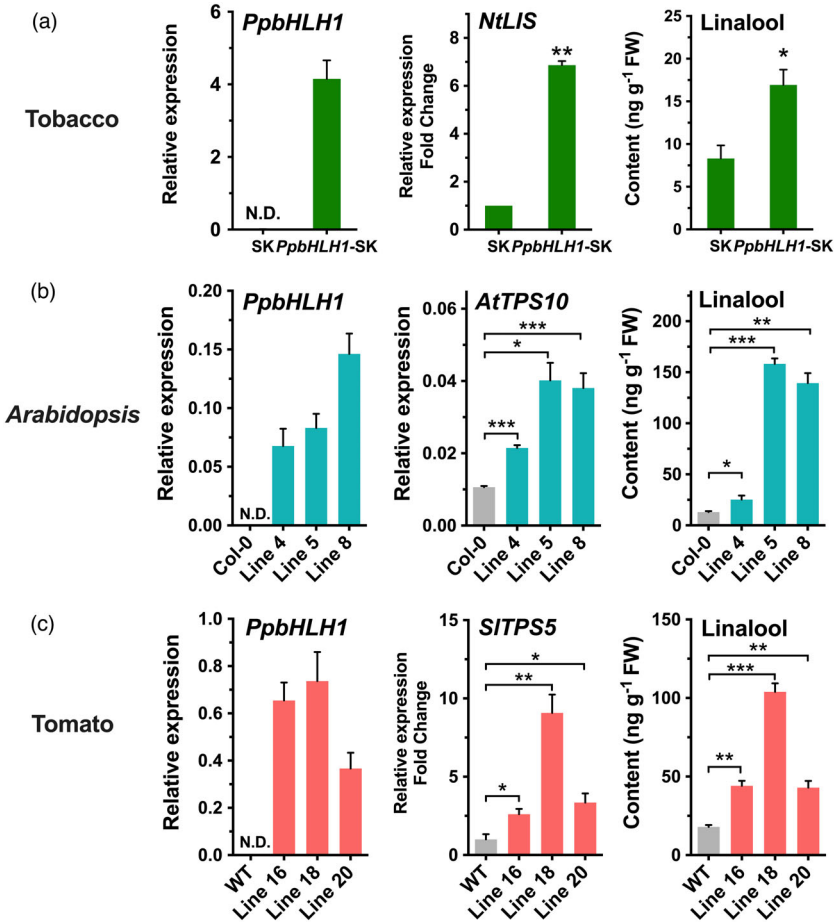

Figure 7 Overexpression of *PpbHLH1* increases content of linalool *in planta*. (a) Transient overexpressing *PpbHLH1* induces linalool accumulation in tobacco (*Nicotiana benthamiana*). (b) Transgenic overexpressing *PpbHLH1* causes linalool accumulation in Arabidopsis. Wild-type Arabidopsis Col-0 was used as control. (c) Transgenic tomato fruits with overexpressing *PpTPS3* produces higher content of linalool than wild-type controls. Relative expression levels were determined using RT-qPCR. Data are presented as mean ± standard error from three independent biological replicates. Significant differences are indicated with asterisks above the bars (*, $P < 0.05$; **, $P < 0.01$; and ***, $P < 0.001$). N.D., not detected.

Engineering of *PpbHLH1* induced linalool synthesis in tobacco, Arabidopsis and tomato fruit

To further confirm the function of PpbHLH1, it was overexpressed in other plant species. For tobacco, leaves were infiltrated with *Agrobacterium* harbouring *PpbHLH1*-pGreen-SK construct, and pGreen-SK vector was used as control. Up-regulating *PpbHLH1* expression increased transcript of tobacco linalool synthase (*NtLIS*, XP_016510950) by sevenfold, accompanying by significant accumulation of linalool (Figure 7a). Compared to wild-type Arabidopsis plants, stable overexpressing *PpbHLH1* significantly enhanced transcript levels of *AtTPS10* and induced contents of linalool in three independent T_2 transgenic lines (Figure 7b). Besides, changes in linalool contents of T_1 transgenic tomatoes were also analysed. For all three lines of transgenic tomato fruits, overexpressing *PpbHLH1* increased *SlTPS5* expression up to eightfold and produced up to fivefold higher contents of linalool compared with the wild-type fruits, respectively (Figure 7c). These results supported that overexpressing peach *PpbHLH1* enhanced linalool production *in planta*.

Discussion

Fruit flavour is determined by a complex mixture of sugars, acids and volatiles including linalool. Monoterpene linalool contributes to a sweet, floral note and is present in many edible fruit species, including guava, plum, pineapple, sweet orange and peach (Lewinsohn *et al*., 2001). Sensory analysis revealed that linalool contributed to consumers' preference of peach fruit (Liu *et al*., 2017; Tian *et al*., 2017). Besides its contribution to flavour, linalool is also an attractant of pollinators and acts as a defence against pathogens and herbivores (Raguso, 2016). Accumulation of linalool induced strong resistance to citrus canker in sweet orange (Shimada *et al*., 2017). Despite its important role during fruit ripening, regulation of linalool synthesis remains largely unclear.

PpTPS3 is a novel synthase regulating linalool synthesis in peach fruit

We initiated study with detecting linalool content during peach fruit ripening and found that linalool accumulated almost exclusively as the enantiomer S-(+)-linalool. The final step for linalool biosynthesis is catalysed by terpene synthase. Among multiple peach *TPS* genes, transcript levels of *PpTPS1* peaked at 94 DAB followed by decline during fruit ripening, whereas *PpTPS3* expression increased throughout fruit development. Here, we showed that PpTPS3 has higher specificity to produce linalool (98.3%) than PpTPS1 (65.1%, Liu *et al*., 2017). Moreover, chiral analysis showed a greater enrichment of S-(+)-linalool (95%) than (R)-(−)-linalool (5%) catalysed by PpTPS3 protein *in vitro*. For PpTPS1, equal ratios of (R)-(−)-linalool and (S)-(+)-linalool were detected for catalysed products (Liu *et al*., 2017). We further validated *PpTPS3* function based on correlationship across peach cultivars, where transcript levels of *PpTPS3* correlate with content of S-(+)-linalool ($R^2 = 0.925$, $P < 0.001$). In addition, overexpressing *PpTPS3* resulted in

significant accumulation, whereas silencing *PpTPS3* led to significant reduction in linalool in peach fruit. Heterologous transgenic tomato fruit further verified the biological function of *PpTPS3* in linalool production. These results indicated that *PpTPS3* is a novel *TPS* gene family member and is associated with S-(+)-linalool synthesis in peach fruit based on both *in vitro* evidence and *in vivo* evidence.

A striking feature found in subcellular localization was the cytoplasm-located PpTPS3. Sequence analysis showed no transit signal peptide of PpTPS3, supporting that its location in the cytoplasm (Figure S9). The biosynthesis of terpenoids depends on the substrate availability of TPS. In general, monoterpene linalool is synthesized in plastids using GPP as precursor. Lots of linalool synthesis-related TPSs had a signal peptide in the N-terminus protein, which guide enzymes into plastids to synthesis linalool (Bohlmann *et al*., 1998), including *AmNES/LIS-2* in snapdragon flowers (Nagegowda *et al*., 2008), *AtTPS10* and *AtTPS14* in Arabidopsis (Ginglinger *et al*., 2013) and *FhTPS1* in *Freesia* × *hybrida* (Gao *et al*., 2018). However, studies suggested that GPP, FPP and their precursors, IPP and DMAPP, can communicate between plastids and cytoplasm through undetermined transporters (Gutensohn *et al*., 2013; Vranová *et al*., 2013). The increase in GPP content in plastids through transgene in tomato led to the metabolic flux of GPP towards cytoplasm, which can be used for monoterpene synthesis (Gutensohn *et al*., 2013). Isozymes of GGPPS were found localized in mitochondria, chloroplasts and endoplasmic reticulum in Arabidopsis, and this allows TPSs to synthesize monoterpenes using GPP in the cytoplasm (Okada *et al*., 2000; Thabet *et al*., 2012). *CoLIS* was found to be mainly responsible for the synthesis of S-(+)-linalool without transit signal peptide in *Cinnamomum osmophloeum* (Lin *et al*., 2013). This provides a new perspective for us to further understand that substrate availability and subcellular localization jointly determine TPS function *in planta*.

Enhanced linalool level by genetic engineering *PpTPS3* upstream regulator PpbHLH1

Recently, TFs that regulate *TPS* expression have been identified in plants (Chuang *et al*., 2018; Yang *et al*., 2020). However, the direct effects of these TFs on linalool synthesis remain undetermined. In this study, peach PpMYB1, PpMYC2, PpWRKY73 and PpEOT1 with the highest homology to FhMYB21L1, SlMYC1, SlWRKY73 and SlEOT1, respectively, failed to activate the *PpTPS3*. To identify TFs associated with linalool synthesis, homologous TFs associated with terpene (monoterpenes, sesquiterpenes and biterpenes) formation were cloned. Moreover, TFs whose expression positively correlated with linalool production during peach fruit ripening were also cloned for screening. After testing 58 TFs, the highest induction of transcription was observed with PpbHLH1. Phylogenetic tree constructed using the sequences of bHLH proteins from both peach and Arabidopsis with some bHLH proteins, which regulate terpenoid formation, showed that PpbHLH1 belongs to the IVa subfamily (Figure S10). A direct effect of PpbHLH1 on expression of the *PpTPS3* and production of linalool was detected in peach fruit with overexpressing and silencing *PpbHLH1*. Moreover, regulatory role of *PpbHLH1* on linalool production was further validated based on significant positive correlations between gene expression and linalool contents across peach cultivars. Besides, a striking feature observed in *PpbHLH1* promoter sequence is the enrichment of light responsiveness. Considering the effect of UV-B light on peach fruit linalool production in our previous study (Liu *et al*., 2017), we here showed that the inhibition of *PpbHLH1* expression was associated with linalool reduction after UV-B irradiation. These results support the conclusion that PpbHLH1 transcriptionally activates the *PpTPS3* gene and formation of volatile linalool in peach fruit.

Having identifying *PpTPS3* and *PpbHLH1* TF, we next tested whether these genes could enhance the levels of linalool in other plants through genetic engineering. Moreover, these genetic engineering experiments could further validate the function of *PpTPS3* and *PpbHLH1* in linalool formation. Indeed, early attempts to engineer plant linalool production mainly focused on *TPS* genes. For instance, heterologous overexpressing linalool synthase gene *LIS* found in *Clarkia breweri* induced accumulation of linalool in tomato fruits (Lewinsohn *et al*., 2001). Transgenic sweet orange plants overexpressing a linalool synthase gene *CuSTS3-1* generated higher levels of linalool in leaves (Shimada *et al*., 2017). Again, our transgenic plants produced significantly higher contents of linalool after engineering peach *PpTPS*3 in both Arabidopsis and tomato fruits. To our best knowledge, no reports have been published in plants engineering linalool production using TFs. Here, the contents of linalool were induced up to 8 and 3 times after overexpressing peach *PpbHLH1* in Arabidopsis and tomato fruits, respectively. Although changed aroma of transgenic tomato fruit could be detected by the human nose, we have not carried out panel tests by tasting. Therefore, the consumers' preference for the transgenic tomato fruit remains unknown.

We previously revealed that linalool is present in fruit as both free and glycosidic bound forms (Wu *et al*., 2019). Besides accumulation of free linalool detected in transgenic plants, significantly higher contents of the linalyl-β-d-glucoside were also observed after the overexpression of *PpTPS3* (Figure S11a). In *PpbHLH1* transgenic tomato fruits, significant increase in the contents of linalyl-β-d-glucoside was observed only in line 18, which has the highest content of free linalool (Figure S11b, Figure 7c). Similar accumulation of glycosylated-bound linalool was also observed in engineered petunia flower (Lücker *et al*., 2001) and Arabidopsis (Aharoni *et al*., 2003) through heterologous overexpressing linalool synthases gene. Besides its contribution to aroma and flavour, linalool is also involved in plant defence. For instance, increased linalool confers strong resistance to citrus canker caused by *Xanthormonas cirti* subsp. *Citri* (Shimada *et al*., 2017). Genetic engineering of linalool metabolism in Arabidopsis and tomato may induce the plant's defence mechanisms, although extra experiments are required.

Notably, a cytotoxic effect of linalool was observed based on increased mitochondrial reactive oxygen species (ROS) and apoptotic cell death caused by high contents of linalool (Cheng *et al*., 2017; Gu *et al*., 2010). These results suggested that high dosages of linalool are toxic to plant cells. Converting free linalool into nonvolatile glycosylated linalool is likely to be a strategy for detoxification in plant (Raguso and Pichersky, 1999). Glycosylation of linalool is catalysed by UGTs, which transfer sugar molecules to linalool (Wu *et al*., 2019). A large part of linalool produced in plants is converted to corresponding conjugated or derivatives, which are stored in tissues instead of releasing (Aharoni *et al*., 2003; Boachon *et al*., 2015). Besides, significant accumulation of *cis*-linalool oxide was detected in transgenic tomato fruit after overexpressing *PpbHLH1* (Figure S11c). Volatile linalool could be further oxidized into nonvolatile defensive chemicals, catalysing by cytochrome P450 enzymes (CYPs) (Boachon *et al*., 2019). Therefore, plants precisely regulate

metabolism of linalool after long-term evolution, including TPS-catalysed biosynthesis, UGT catalysed glycosylation and CYP-mediated oxidation. Correspondingly, plants regulate linalool content, making fruit attractive to seed-dispersing animals, while reducing potential toxic effects of free linalool.

Peach fruit linalool synthesis is regulated not only by TF bHLH

Besides bHLH IVa subfamily, we also found three TFs, PpNAC1, PpNAC2 and PpERF61, with activation effect on *PpTPS3* transcription (Figure 4a). It has been reported that PpNAC1 and PpNAC2 were associated with anthocyanin biosynthesis in peach (Zhou *et al*., 2015), suggesting that these two NACs play an important role in regulating peach secondary metabolism. Moreover, homologous NAC proteins in kiwifruit activate *AaTPS1* transcription and thereby regulate monoterpene biosynthesis (Nieuwenhuizen *et al*., 2015). Transcript levels of *PpERF61* were positively related to *PpTPS3* expression during peach fruit ripening ($R > 0.5$), implying it might be an activator of linalool biosynthesis. Volatile linalool is a major contributor to flavour, therefore plays an important role for fruit consumption and help seed dispersal. Considering the important role of linalool has in plants and fruits, it seems reasonable to speculate that transcription of *PpTPS3* may be regulated by multiple TFs in peach.

DNA methylation is one of the epigenetic modifications that play a critical role in fruit development and ripening (Tang *et al*., 2020). Although early DNA methylation studies were limited to model fruit tomato (Zhong *et al*., 2013), the increasing number of crop genomes has facilitated the DNA methylation studies in fruit crops such as orange (Huang *et al*., 2019), strawberry (Cheng *et al*., 2018), apple (Xu *et al*., 2018) and peach fruit (Zhu *et al*., 2020). In tomato fruit, changes in DNA methylation levels in the promoters of genes are associated with the production of flavour-related chemicals including volatiles (Zhang *et al*., 2016, 2020). Here, decreased DNA methylation was observed during peach fruit ripening, accompanying by increased *PpTPS3* expression and high accumulated linalool contents. High DNA methylation may reduce *PpTPS3* expression and produce trace linalool to protect immature seeds of peach fruit. For ripe peach fruit, reduced DNA methylation may contribute to *PpTPS3* expression and linalool accumulation, therefore making ripe fruit more attractive to consumers. To our best knowledge, this is the first study reporting fruit linalool synthesis is related to DNA methylation. It is possible that epigenetic regulation methylation is an added level of insurance for regulating linalool production during peach fruit ripening.

Conclusions

Accumulation of linalool during fruit ripening is important for fruit consumption and for seed dispersal. Here, we cloned and characterized a novel gene *PpTPS3* encoding a protein capable of converting GPP to acyclic monoterpene linalool based on both *in vitro* and *in vivo* experiments. TF PpbHLH1 activates *PpTPS3* transcription via binding to its promoter. Overexpressing *PpbHLH1* enhances linalool, and silencing this gene reduces linalool content in peach fruit. Metabolic engineering of linalool production was generated by overexpression of *PpbHLH1* in multiple plants such as Arabidopsis and tomato fruits. Moreover, our results showed that linalool accumulation is associated with DNA methylation of synthesis gene. Our study showed that linalool production is regulated not only by TFs, but also by epigenetic modifications during fruit ripening. Knowledge of how volatile pathways are regulated would greatly facilitate efforts to improve fruit flavour quality.

Methods

Plant materials and treatment

Peach (*Prunus persica* L. Batsch cv. Hujingmilu) fruits were obtained from the Melting Peach Research Institute of Fenghua, Zhejiang Province, China. They were harvested at five developmental stages, S1 (first rapid growth phase, 34 days after bloom, DAB), S2 (stone hardening, 71 DAB), S3 (second rapid growth phase, 94 DAB), S4 (mature stage, 108 DAB) and S5 (ripening stage, 111 DAB) (Wu *et al*., 2019). Peach fruits were exposed to 1.5 w/m^2 UV-B irradiation for 6 h and 48 h at 20 °C (Liu *et al*., 2017). Moreover, fruits of nine natural peach cultivars (*Prunus persica*) were sampled at the ripening stage, namely 'Guanghetao' (GHT), 'Honggengansutao' (HGGST), 'Honghuashantao' (HHST), 'Zaoshanghaishuimi' (ZSHSM), 'Fuyangchiyue' (FYCY), 'Hongpan1' (HP1), 'Hongpan2' (HP2), 'Hujingmilu' (HJML) and 'Danxia' (DX). Three biological replicates with five fruits each were sampled, frozen in liquid nitrogen and stored at −80 °C for further use.

Volatiles analysis by GC-MS

Volatiles were analysed according to our previous study (Wu *et al*., 2019). Frozen peach fruit (5 g), peel (1 g), tomato fruit (5 g) and leaf (1 g), Arabidopsis (1 g) and tobacco leaf (1 g) were ground into powder under liquid nitrogen and transferred to vials containing 200 mM ethylenediaminetetraacetic acid (EDTA) and 20% $CaCl_2$ solution. Before the vials were sealed, 30 μL 2-octanol (0.8 mg/mL) was added as internal standard. A fibre coated with 65 μm of polydimethylsiloxane and divinylbenzene (PDMS−DVB) (Supeclo Co., Bellefonte, PA) was used for volatile collection. The vials were placed in the tray of a solid-phase microextraction (SPME) autosampler (Combi PAL, CTC Analytics, Agilent Technologies), coupled to an Agilent 7890N gas chromatograph and an Agilent 5975C mass spectrometer. Volatiles were separated on a DB-WAX column (30 m × 0.25 mm i.d. × 0.25 μm film thickness; J & W Scientific, Folsom, CA). Carrier gas helium rate was 1.0 mL/min. The temperature programme started at 40 °C and was increased by 3 °C/min to 100 °C and then to 245 °C at 5 °C/min. The column effluent was ionized by electron ionization at an energy of 70 eV with a transfer temperature of 250 °C and a source temperature of 230 °C. Volatiles were identified by comparing their electron ionization mass spectra with the NIST Mass Spectral Library (NIST-08) and the retention time of authentic standards. Quantification of volatiles was performed using the peak area of the internal standard as a reference based on total ion chromatogram. Extraction and hydrolysis of glycosylated volatiles were performed according to Wu *et al*. (2019).

Chiral GC-MS analysis

Chiral GC-MS analysis was performed using a 7890A gas chromatograph coupled to an Agilent 5975C mass spectrometer. Helium was used as carrier gas. The enantiomers of linalool were separated with a β-Dex™ 325 capillary column (30 m × 0.25 mm × 0.25 μm; Supelco Co.) according to methods described by Liu *et al*. (2017). The initial oven temperature was 35 °C, held for 1 min, increased to 118 °C by 5 °C/min, then increased to 118.4 °C and followed by a further increase to 230 °C by 5 °C/min. Authentic standards (Sigma-Aldrich) were used for identification of linalool enantiomers.

Heterologous expression in *Escherichia coli* and enzymatic activity assay

Recombinant protein purification was performed following the method described previously (Wu *et al*., 2019). The full-length cDNA of the *PpTPS3* gene was inserted into the pET6 × HN expression vector (Clontech, Mountain View, CA) using the primers in Table S9. After sequence validation, pET vector was transformed into *Escherichia coli* BL21 (DE3) pLysS (Promega, Madison, WI). Recombinant protein was purified by the HisTALON™ gravity column (Clontech) following the manufacturer's instructions and replaced with Tris-HCl buffer (100 mM Tris, 2 mM DTT, pH 7.5) by the PD-10 Desalting Column (GE Healthcare). SDS-PAGE was performed, and the protein was visualized by Coomassie Brilliant Blue. Enzymatic activity assay was carried out according to Liu *et al*. (2017). Enzyme assay buffer B (50 mM HEPES, 7.5 mM $MgCl_2$, 100 mM KCl, 5 mM dithiothreitol and 10% (v/v) glycerol, pH 7.0) used in the reaction with geranyl pyrophosphate (GPP) as substrate. The reaction was performed at 4-mL sealed glass bottle, 200 μL of purified protein, 10 μg of reaction substrate and 800 μL of enzyme reaction buffer were added to 1 mL of the reaction system, and after adding 5 μL (0.2 mg/mL) of 2-octanol as an internal standard, the reaction was performed at 42 °C for 15 min. The protein expressed by the empty vector and the substrate were heated separately as a negative control. The product catalysed by the enzyme was collected by SPME before GC-MS analysis.

Gene expression analysis

Total RNA was extracted according to the protocol described by Zhang *et al*. (2006), and libraries for high-throughput Illumina strand-specific RNA-seq were prepared as described previously (Zhang *et al*., 2016). RNA-seq raw data used for the present study can be found in the National Center for Biotechnology Information (NCBI) Short Read Archive database. Accession Numbers PRJNA576753 and SRP103523 are for peach samples at different development and ripening stages and under UV-B treatment, respectively. For quantitative reverse-transcription PCR (RT-qPCR) analysis, PrimeScript RT Reagent Kit with gDNA Eraser (Takara) was used to synthesize the first-strand cDNA, and then, experiments were performed using CFX96 instrument (Bio-Rad, Hercules, CA) and SsoFast EvaGreen Supermix (Bio-Rad). Each RT-qPCR analysis contains three replicates. Oligonucleotide primers used for RT-qPCR analysis are listed in Table S9.

Dual-luciferase assays

According to the previous protocol (Zhang *et al*., 2018), full-length cDNAs of transcription factors were cloned into pGreen II 0029 62-SK vector, and the promoter of *PpTPS3* was cloned into pGreen II 0800-LUC vector using the primers listed in Tables S4, S8 and S9. The above constructs were transformed into *Agrobacterium tumefaciens* GV3101::pSoup using the Gene Pulser Xcell™ Electroporation Systems (Bio-Rad, Hercules, CA). To obtain the activity of a specific transcription factor on the *PpTPS3* promoter, the *Agrobacterium* culture mixtures were comprised of 1 mL TFs and 100 μL promoter for transient expression in *Nicotiana benthamiana* leaves. The ratio of enzyme activities of firefly luciferase (LUC) and Renilla luciferase (REN) was measured using a Modulus Luminometer (Promega, Madison, WI) on the third day after infiltration. Enzyme activities of LUC and REN were assayed using dual-luciferase assay reagents (Promega). The LUC/REN value of the empty vector SK on the promoter was set as 1, as a calibrator. For each transcription factor–promoter interaction, at least three independent experiments were performed, with six replicates in each experiment.

Yeast one-hybrid assay

The sequence of the *PpTPS3* promoter was cloned into the pAbAi vector, and the construct was integrated into the genome of the Y1HGold yeast strain. The background aureobasidin A resistance (AbA^r) expression of Y1HGold *PpTPS3*-pAbAi strain was tested on selective synthetic dextrose medium (SD) uracil. Then, the full length of PpbHLH1 was cloned into the pGADT7 vector for identification. After determining the minimal inhibitory concentration of AbA for the bait strains, the AD prey vectors were transformed into the bait strain and screened on an SD/-Leu/AbA plate. Autoactivation and transcription factor–promoter interaction analysis were conducted according to the Matchmaker® Gold Yeast One-Hybrid Library Screening System (Clontech) manufacturer's protocol. All transformations and screenings were performed at least three times. Primers used in this assay are listed in Table S9.

Electrophoretic mobility shift assay (EMSA)

The coding sequence of PpbHLH1 was cloned into the pGEX-4T-1 vector using the primers listed in Table S9 and then was expressed in *Escherichia coli* BL21. Expression and purification of the recombinant protein were performed according to GST-tag Protein Purification Kit (Beyotime) manufacturer's instructions. The EMSA was conducted using the LightShift® Chemiluminescent EMSA Kit (Thermo Fisher Scientific). The details of the EMSA are provided by Li *et al*. (2017). The double-stranded probes were made by annealing separately synthesized strands, with 3′ biotin labelling. The probes used for EMSAs are listed in Table S9.

Gene transient overexpression in peach fruit

Transient overexpression in peach fruit was performed according to our previous study (Liu *et al*., 2017). Constructs were electroporated into *Agrobacterium tumefaciens* GV3101 and activated at 28 °C until the OD_{600} reached 0.8–1.0. After disinfecting the surface of the peach fruit, two flesh cubes (1 cm thick) were taken from opposite sides of each fruit. Each piece was cut into two halves on average, and *A. tumefaciens* carrying the *PpTPS3* or *PpbHLH1* construct and *A. tumefaciens* carrying empty construct were infiltrated under a −70 kPa vacuum, respectively. After vacuum infiltration, flesh cubes were rinsed three times with sterile water and cultured on Murashige and Skoog (MS) medium in a growth chamber (20 °C, RH 85%) for 3 day. Flesh cubes were then sampled for GC-MS analysis. Transient expression treatments were repeated three times with five fruits each.

TRV-based virus-induced gene silencing (VIGS) in peach

Virus-induced gene silencing was performed according to previous study (Zhao *et al*., 2020). *Agrobacterium* cells expressing pTRV1 and pTRV2 or pTRV2-*PpPDS*/*PpTPS3*/*PpbHLH1* constructs were cultured to an OD_{600} of 0.5–0.8, and then, *Agrobacterium* cells were collected by centrifugation and resuspended in 1/2 volume of MES infiltration buffer (200 mM acetosyringone, 10 mM $MgCl_2$, 10 mM MES; pH 5.6). *Agrobacterium* with pTRV1 and pTRV2 constructs were mixed in a ratio of 1:1 and infiltrated using syringes into the flesh of peach fruit on the trees. Three biological replicates with ten fruits each were sampled for analysis.

Stable overexpression in tomato fruit

Full-length cDNAs of *PpTPS3* and *PpbHLH1* were cloned into pBI121 vector or pBIN19-E8, respectively, using the primers listed in Table S9. *A. tumefaciens*-mediated *tomato (cv MicroTom) transformation was performed according to Wang et al*. (2005). The identified T_1 generation of transgenic and wild-type (WT) tomato plants were grown in a greenhouse (25 °C, 16-h light/8-h darkness). Tomato fruits at red ripe stage (breaker + 7 days) were frozen in liquid nitrogen and stored at −80 °C for analysis. Three tomato plants were selected from each line as three biological replicates, and each replicate contained five fruits.

Stable transformation of Arabidopsis

Four-week-old seedlings of Arabidopsis plants were transformed according to the floral dip method (Clough and Bent, 1998). *PpTPS3*-pBI121 constructs were used to transform *tps10* mutant in the Columbia-0 genetic background, and *PpbHLH1*-pBI121 was transformed in the wild-type (WT) background. The homozygous Arabidopsis mutant (SALK_041114C) was purchased from the Arabidopsis Information Resource (TAIR). Transgenic seeds were selected on 1/2 Murashige and Skoog medium with 50 mg/L kanamycin, and the 1 month of whole plants (T_2 and WT) was harvested and analysed.

DNA methylation analysis

DNeasy Plant Mini Kit (Qiagen, Hilden, Germany) was used for genomic DNA extraction from peach fruit samples. DNA quality was monitored by agarose gel electrophoresis and a ratio of A260/A280. Genomic DNA with bisulphite conversion rates higher than 99.5% was used for Illumina DNA sequencing. A HiSeq 2500 was used for DNA sequencing according to Illumina protocols. Methylome data at single-base resolution were achieved, and occurrence of DNA methylation was analysed according to our previous study (Zhang *et al*., 2016).

Subcellular localization analysis

The recombined GFP vectors were constructed using primers listed in Table S9 and were electroporated into *A. tumefaciens* GV3101 for transient expression in tobacco (*N. benthamiana*) leaves. After 48 h, leaves were detached for analysis using a confocal laser scanning microscope (LSM 780; Carl Zeiss, Oberkochen, Germany). Images were processed with the LSM Image Browser (Carl Zeiss). Protoplast extraction was performed using the plant protoplast preparation and transformation kit (RTU4052) (Real-Times, China) following the manufacturer's protocol.

Statistics

Figures were produced using GraphPad Prism 7.0 (GraphPad Software; San Diego, CA). The two-sample significance test was calculated using unpaired Student's *t* test (*, $P < 0.05$; **, $P < 0.01$; and ***, $P < 0.001$) (SPSS 19.0; SPSS Inc., Chicago, IL). MetaboAnalyst 4.0 was used for correlation analysis in the present study.

Acknowledgements

This research was supported by the National Key R & D Program of China (2016YFD0400101), the National Natural Science Foundation of China (31972379) and the Fundamental Research Funds for the Zhejiang Provincial Universities (2021XZZX026).

Conflict of Interest Statement

The authors declare that they have no conflict of interest.

Author contributions

B.Z. conceived the research plans; C.W. and H.L. performed most of the experiments and analyses with help from X.C. and M.Z.; C.W. and B.Z. wrote the article; and B.Z., X.L. and K.C. reviewed and edited the manuscript. All authors have read and approved to the published version of the manuscript.

References

Aharoni, A., Giri, A.P., Deuerlein, S., Griepink, F., de Kogel, W.J., Verstappen, F.W., Verhoeven, H.A. *et al*. (2003) Terpenoid metabolism in wild-type and transgenic Arabidopsis plants. *Plant Cell,* **15**, 2866–2884.

Aharoni, A., Giri, A., Verstappen, F.W.A., Bertea, C.M., Sevenier, R., Sun, Z., Jongsma, M.A. *et al*. (2004) Gain and loss of fruit flavor compounds produced by wild and cultivated strawberry species. *Plant Cell,* **16**, 3110–3131.

Boachon, B., Burdloff, Y., Ruan, J.X., Rojo, R., Junker, R.R., Vincent, B., Nicolè, F. *et al*. (2019) A promiscuous CYP706A3 reduces terpene volatile emission from Arabidopsis flowers, affecting florivores and the floral microbiome. *Plant Cell,* **31**, 2947–2972.

Boachon, B., Junker, R.R., Miesch, L., Bassard, J.E., Höfer, R., Caillieaudeaux, R., Seidel, D.E. *et al*. (2015) CYP76C1(Cytochrome P450)-mediated linalool metabolism and the formation of volatile and soluble linalool oxides in Arabidopsis flowers: A strategy for defense against floral antagonists. *Plant Cell,* **27**, 2972–2990.

Bohlmann, J., Meyer-Gauen, G. and Croteau, R. (1998) Plant terpenoid synthases: molecular biology and phylogenetic analysis. *Proc. Natl. Acad. Sci. USA,* **95**, 4126–4133.

Bonnländer, B., Cappuccio, R., Liverani, F.S. and Winterhalter, P. (2006) Analysis of enantiomeric linalool ratio in green and roasted coffee. *Flavour Frag. J.* **21**, 637–641.

Chen, F., Tholl, D., D'Auria, J.C., Farooq, A., Pichersky, E. and Gershenzon, J. (2003) Biosynthesis and emission of terpenoid volatiles from Arabidopsis flowers. *Plant Cell,* **15**, 481–494.

Cheng, J.F., Niu, Q.F., Zhang, B., Chen, K.S., Yang, R.H., Zhu, J.K., Zhang, Y.J. *et al*. (2018) Downregulation of RdDM during strawberry fruit ripening. *Genome Biol.* **19**, 212.

Cheng, Y.H., Dai, C. and Zhang, J. (2017) SIRT3–SOD2–ROS pathway is involved in linalool-induced glioma cell apoptotic death. *Acta Biochim. Pol.* **64**, 343–350.

Chuang, Y.C., Hung, Y.C., Tsai, W.C., Chen, W.H. and Chen, H.H. (2018) PbbHLH4 regulates floral monoterpene biosynthesis in *Phalaenopsis* orchids. *J. Exp. Bot.* **69**, 4363–4377.

Clough, S.J. and Bent, A.F. (1998) Floral dip: a simplified method for Agrobacterium-mediated transformation of *Arabidopsis thaliana*. *Plant J.* **16**, 735–743.

Eduardo, I., Chietera, G., Bassi, D., Rossini, L. and Vecchietti, A. (2010) Identification of key odor volatile compounds in the essential oil of nine peach accessions. *J. Sci. Food Agric.* **90**, 1146–1154.

Falara, V., Akhtar, T.A., Nguyen, T.T.H., Spyropoulou, E.A., Bleeker, P.M., Schauvinhold, I., Matsuba, Y. *et al*. (2011) The tomato terpene synthase gene family. *Plant Physiol.* **157**, 770–789.

Gao, F., Liu, B., Li, M., Gao, X.Y., Fang, Q., Liu, C., Ding, H. *et al*. (2018) Identification and characterization of terpene synthase genes accounting for volatile terpene emissions in flowers of *Freesia* × *hybrida*. *J. Exp. Bot.* **69**, 4249–4265.

Ginglinger, J.F., Boachon, B., Höfer, R., Paetz, C., Köllner, T.G., Miesch, L., Lugan, R. *et al*. (2013) Gene coexpression analysis reveals complex metabolism of the monoterpene alcohol linalool in Arabidopsis flowers. *Plant Cell,* **25**, 4640–4657.

Gu, Y., Ting, Z., Qiu, X., Zhang, X.Z., Gan, X.X., Fang, Y.M., Xu, X.H. *et al*. (2010) Linalool preferentially induces robust apoptosis of a variety of leukemia cells via upregulating p53 and cyclin-dependent kinase inhibitors. *Toxicology,* **268**, 19–24.

Gutensohn, M., Orlova, I., Nguyen, T.T.H., Davidovich-Rikanati, R., Ferruzzi, M.G., Sitrit, Y., Lewinsohn, E. *et al*. (2013) Cytosolic monoterpene biosynthesis is supported by plastid-generated geranyl diphosphate substrate in transgenic tomato fruits. *Plant J.* **75**, 351–363.

He, J., Fandino, R.A., Halitschke, R., Luck, K., Köllner, T.G., Murdock, M.H., Ray, R. *et al*. (2019) An unbiased approach elucidates variation in (S)-(+)-linalool, a context-specific mediator of a tri-trophic interaction in wild tobacco. *Proc. Natl. Acad. Sci. USA,* **116**, 14651–14660.

Higo, K., Ugawa, Y., Iwamoto, M. and Korenaga, T. (1999) Plant cis-acting regulatory DNA elements (PLACE) database. *Nucleic Acids Res.* **27**, 297–300.

Huang, H., Liu, R.E., Niu, Q.F., Tang, K., Zhang, B., Zhang, H., Chen, K.S. *et al*. (2019) Global increase in DNA methylation during orange fruit development and ripening. *Proc. Natl. Acad. Sci. USA,* **116**, 1430–1436.

Huang, X.Z., Xiao, Y.T., Köllner, T.G., Jing, W.X., Kou, J.F., Chen, J.Y., Liu, D.F. *et al*. (2017) The terpene synthase gene family in *Gossypium hirsutum* harbors a linalool synthase GhTPS12 implicated in direct defence responses against herbivores. *Plant Cell Environ.* **41**, 261–274.

Klee, H.J. and Tieman, D.M. (2018) The genetics of fruit flavour preferences. *Nat. Rev. Genet.* **19**, 347–356.

Kumar, Y., Khan, F., Rastogi, S. and Shasany, A.K. (2018) Genome-wide detection of terpene synthase genes in holy basil (*Ocimum sanctum* L.). *PLoS One,* **13**, e0207097.

Lewinsohn, E., Schalechet, F., Wilkinson, J., Matsui, K., Tadmor, Y., Nam, K.H., Amar, O. *et al*. (2001) Enhanced levels of the aroma and flavor compound S-linalool by metabolic engineering of the terpenoid pathway in tomato fruits. *Plant Physiol.* **127**, 1256–1265.

Li, X., Xu, Y.Y., Shen, S.L., Yin, X.R., Klee, H., Zhang, B., Chen, K.S. *et al*. (2017) Transcription factor CitERF71 activates the terpene synthase gene CitTPS16 involved in the synthesis of E-geraniol in sweet orange fruit. *J. Exp. Bot.* **68**, 4929–4938.

Lin, Y.L., Lee, Y.R., Huang, W.K., Chang, S.T. and Chu, F.H. (2013) Characterization of S-(+)-linalool synthase from several provenances of *Cinnamomum osmophloeum*. *Tree Genet. Genomes,* **10**, 75–86.

Liu, H.R., Cao, X.M., Liu, X.H., Xin, R., Wang, J.J., Gao, J., Wu, B.P. *et al*. (2017) UV-B irradiation differentially regulates terpene synthases and terpene content of peach. *Plant Cell Environ.* **40**, 2261–2275.

Lücker, J., Bouwmeester, H.J., Schwab, W., Blaas, J., van der Plas, L.H. and Verhoeven, H.A. (2001) Expression of *Clarkia S*-linalool *synthase in transgenic petunia plants results in the accumulation of S-linalyl-beta-d-glucopyranoside. Plant J.* **27**, 315–324.

Magnard, J.-L., Bony, A.R., Bettini, F., Campanaro, A., Blerot, B., Baudino, S. and Jullien, F. (2018) Linalool and linalool nerolidol synthases in roses, several genes for little scent. *Plant Physiol. Biochem.* **127**, 74–87.

Martin, D.M., Aubourg, S., Schouwey, M.B., Daviet, L., Schalk, M., Toub, O., Lund, S.T. *et al*. (2010) Functional annotation, genome organization and phylogeny of the grapevine (*Vitis vinifera*) terpene synthase gene family based on genome assembly, FLcDNA cloning, and enzyme assays. *BMC Plant Biol.* **10**, 226.

Nagegowda, D.A., Gutensohn, M., Wilkerson, C.G. and Dudareva, N. (2008) Two nearly identical terpene synthases catalyze the formation of nerolidol and linalool in snapdragon flowers. *Plant J.* **55**, 224–239.

Nieuwenhuizen, N.J., Chen, X., Wang, M.Y., Matich, A.J., Perez, R.L., Allan, A.C., Green, S.A. *et al*. (2015) Natural variation in monoterpene synthesis in kiwifruit: transcriptional regulation of terpene synthases by NAC and ETHYLENE-INSENSITIVE3-like transcription factors. *Plant Physiol.* **167**, 1243–1258.

Nieuwenhuizen, N.J., Green, S.A., Chen, X.Y., Bailleul, E.J.D., Matich, A.J., Wang, M.Y. and Atkinson, R.G. (2013) Functional genomics reveals that a compact terpene synthase gene family can account for terpene volatile production in apple. *Plant Physiol.* **161**, 787–804.

Okada, K., Saito, T., Nakagawa, T., Kawamukai, M. and Kamiya, Y. (2000) Five geranylgeranyl diphosphate synthases expressed in different organs are localized into three subcellular compartments in Arabidopsis. *Plant Physiol.* **122**, 1045–1056.

Raguso, R.A. (2016) More lessons from linalool: insights gained from a ubiquitous floral volatile. *Curr. Opin. Plant Biol.* **32**, 31–36.

Raguso, R. and Pichersky, E. (1999) A day in the life of a linalool molecule: chemical communication in a plant–pollinator system. Part 1: linalool biosynthesis in flowering plants. *Plant Spec. Biol.* **14**, 95–120.

Ravid, U., Putievsky, E., Weinstein, V. and Ikan, R. (1985) Determination of the enantiomeric composition of natural flavouring agents by ^{1}H-NMR spectroscopy. In *Essential Oils and Aromatic Plants* (Baerheim Svendsen, A. and Scheffer, J.J.C., eds.), pp. 135–138. The Netherlands: Springer.

Ravid, U., Putievsky, E., Katzir, I. and Lewinsohn, E. (1997) Enantiomeric composition of linalool in the essential oils of *Ocimum* species and in commercial basil oils. *Flavour Frag. J.* **12**, 293–296.

Shimada, T., Endo, T., Rodríguez, A., Fujii, H., Goto, S., Matsuura, T., Hojo, Y. *et al*. (2017) Ectopic accumulation of linalool confers resistance to *Xanthomonas citri* subsp. *citri* in transgenic sweet orange plants. *Tree Physiol.* **37**, 654–664.

Spyropoulou, E.A., Haring, M.A. and Schuurink, R.C. (2014) RNA sequencing on *Solanum lycopersicum* trichomes identifies transcription factors that activate terpene synthase promoters. *BMC Genom.* **15**, 402.

Tang, D.G., Gallusci, P. and Lang, Z.B. (2020) Fruit development and epigenetic modifications. *New Phytol.* **228**, 839–844.

Thabet, I., Guirimand, G., Guihur, A., Lanoue, A., Courdavault, V., Papon, N., Bouzid, S. *et al*. (2012) Characterization and subcellular localization of geranylgeranyl diphosphate synthase from *Catharanthus roseus*. *Mol. Biol. Rep.* **39**, 3235–3243.

Tian, H.L., Wang, P., Zhan, P., Yan, H.Y., Zhou, W.J. and Zhang, F. (2017) Effects of β-glucosidase on the aroma characteristics of flat peach juice as assessed by descriptive sensory analysis and gas chromatography and compared by partial least squares regression. *LWT-Food Sci. Technol.* **82**, 113–120.

Vranová, E., Coman, D. and Gruissem, W. (2012) Structure and dynamics of the isoprenoid pathway network. *Mol. Plant.* **5**, 318–333.

Vranová, E., Coman, D. and Gruissem, W. (2013) Network analysis of the MVA and MEP pathways for isoprenoid synthesis. *Annu. Rev. Plant Biol.* **64**, 665–700.

Wang, H., Jones, B., Li, Z., Frasse, P., Delalande, C., Regad, F., Chaabouni, S. *et al*. (2005) The tomato Aux/IAA transcription factor IAA9 is involved in fruit development and leaf morphogenesis. *Plant Cell,* **17**, 2676–2692.

Wu, B.P., Cao, X.M., Liu, H.R., Zhu, C.Q., Klee, H.J., Zhang, B. and Chen, K.S. (2019) UDP-glucosyltransferase *PpUGT85A2* controls volatile glycosylation in peach. *J. Exp. Bot.* **70**, 925–936.

Xu, J.D., Zhou, S.S., Gong, X.Q., Song, Y., van Nocker, S., Ma, F.W. and Guan, Q.M. (2018) Single-base methylome analysis reveals dynamic epigenomic differences associated with water deficit in apple. *Plant Biotechnol. J.* **16**, 672–687.

Yang, Z.Z., Li, Y.Q., Gao, F.Z., Jin, W., Li, S.Y., Kimani, S., Yang, S. *et al*. (2020) MYB21 interacts with MYC2 to control the expression of terpene synthase genes in flowers of *Freesia hybrida* and *Arabidopsis thaliana*. *J. Exp. Bot.* **71**, 4140–4158.

Zhang, B., Chen, K.S., Bowen, J., Allan, A., Espley, R., Karunairetnam, S. and Ferguson, I. (2006) Differential expression within the LOX gene family in ripening kiwifruit. *J. Exp. Bot.* **57**, 3825–3836.

Zhang, B., Tieman, D.M., Jiao, C., Xu, Y.M., Chen, K.S., Fei, Z.J., Giovannoni, J.J. *et al*. (2016) Chilling-induced tomato flavor loss is associated with altered volatile synthesis and transient changes in DNA methylation. *Proc. Natl. Acad. Sci. USA,* **113**, 12580–12585.

Zhang, C., Duan, W.Y., Chen, K.S. and Zhang, B. (2020) Transcriptome and methylome analysis reveals effects of ripening on and off the vine on flavor quality of tomato fruit. *Postharvest Biol. Technol.* **162**, 111096.

Zhang, Y.Y., Yin, X.R., Xiao, Y.W., Zhang, Z.Y., Li, S.J., Liu, X.F., Zhang, B. *et al*. (2018) An ETHYLENE RESPONSE FACTOR-MYB transcription complex regulates furaneol biosynthesis by activating QUINONE OXIDOREDUCTASE Expression in Strawberry. *Plant Physiol.* **178**, 189–201.

Zhao, Y., Dong, W.Q., Zhu, Y.C., Allan, A.C., Wang, K.L. and Xu, C.J. (2020) *PpGST1*, an anthocyanin-related glutathione S-transferase gene, is essential for fruit coloration in peach. *Plant Biotechnol. J.* **18**, 1284–1295.

Zhong, S.L., Fei, Z.J., Chen, Y.R., Zheng, Y., Huang, M.Y., Vrebalov, J., McQuinn, R. *et al*. (2013) Single-base resolution methylomes of tomato fruit development reveal epigenome modifications associated with ripening. *Nat. Biotechnol.* **31**, 154–159.

Zhou, H., Lin-Wang, K., Wang, H.L., Gu, C., Dare, A.P., Espley, R.V., He, H.P. *et al*. (2015) Molecular genetics of blood-fleshed peach reveals activation of anthocyanin biosynthesis by NAC transcription factors. *Plant J.* **82**, 105–121.

Zhu, H., Xia, R., Zhao, B.Y., An, Y.Q., Dardick, C.D., Callahan, A.M. and Liu, Z.R. (2012) Unique expression, processing regulation, and regulatory network of peach (*Prunus persica*) miRNAs. *BMC Plant Biol.* **12**, 149–167.

Zhu, Y.C., Zhang, B., Allan, A.C., Lin-Wang, K., Zhao, Y., Wang, K., Chen, K.S. *et al*. (2020) DNA demethylation is involved in the regulation of temperature-dependent anthocyanin accumulation in peach. *Plant J.* **102**, 965–976.

Supporting information

Additional supporting information may be found online in the Supporting Information section at the end of the article.

Figure S1 Alignment of amino acid sequences of 38 peach PpTPSs.
Figure S2 SDS-PAGE analysis of PpTPS3 protein.
Figure S3 Silencing *PpPDS* (Prupe.1G174100) gene in peach fruit.
Figure S4 Expression of *AtTPS10* and *AtTPS14* in *PpTPS3* transgenic Arabidopsis.
Figure S5 Changes in content of free linalool in *PpTPS3* transgenic tomato leaves.
Figure S6 Expression profiles of three *bHLH* genes and regulatory effect of PpbHLH1 on the promoter of *PpTPS1*.
Figure S7 PpbHLH1 binds to *PpTPS3* promoter.
Figure S8 Correlation between transcript and S-(+)-Linalool content in different peach cultivars.
Figure S9 Alignment of amino acid sequence of *PpTPS3* with closely related sequences from TPS-g subfamily.
Figure S10 Phylogenetic tree constructed using the sequences of bHLH proteins from both peach and Arabidopsis with some bHLH proteins which regulate linalool or terpene formation in other species.
Figure S11 Changes in content of linalyl-β-d-glucoside and linalool oxide in *PpTPS3* and *PpbHLH1* transgenic tomato fruits.
Table S1 Content of volatiles in peach fruit during development and ripening.
Table S2 Accession numbers for plant TPSs used for sequence analysis in Figure 2.
Table S3 Peach homologues of transcription factors that regulate terpenoid formation.
Table S4 Primers of TFs which have expression correlation with *PpTPS3* during peach fruit ripening.
Table S5 The light response-related *cis*-acting elements of *PpbHLH1* promoter.
Table S6 Statistic of whole-genome bisulfite sequencing reads from peach fruit at different development stages and under UV-B treatment.
Table S7 Statistic of sequencing depth and covering in peach fruit at different development stages and under UV-B treatment.
Table S8 Primers of TFs which homologues of transcription factors that regulate terpenoid formation.
Table S9 Other primer sequences used in the present study.